Biochimica et Biophysica Acta, 945 (1988) 253–262
Elsevier

BBA 74202

Fluorescence analysis of size distribution and mode of dye release from carboxyfluorescein-loaded vesicles: application to the study of complement–membrane interactions *

Zi-Yao Liu, Rikki Solow ** and Valerie W. Hu **

Department of Biochemistry, Uniformed Services University of the Health Sciences, Bethesda, MD (U.S.A.)

(Received 19 April 1988)
(Revised manuscript received 26 July 1988)

Key words: Carboxyfluorescein-loaded vesicle; Size distribution; Vesicle aggregation; Complement-induced permeability; Permeability; Dye release

We wish to report a novel method for visualizing large unilamellar vesicles loaded with a fluorescent dye and for monitoring changes in the size distribution as well as state of aggregation of such dye-loaded liposomes. In addition, we demonstrate that this method can be used to distinguish between all-or-none release of dye and graded release of dye from individual vesicles. Using this technique, we have characterized complement-mediated release of carboxyfluorescein from large unilamellar vesicles and have found that C5–8 complexes mediate a graded release of dye while C5–9 complexes cause an all-or-none release. Furthermore, complement appears to preferentially attack the medium to larger-sized vesicles in our population of large unilamellar vesicles while smaller vesicles appear to be selectively spared.

Introduction

Carboxyfluorescein-loaded vesicles have been frequently used to probe liposome–protein, liposome–liposome, and liposome–cell interactions [1–8]. In particular, release of this dye marker from liposomes has been taken as an indication of pore formation or perturbation of membrane structure by various cytotoxic proteins [7–9]. The use of entrapped dye at self-quenching concentrations allows continuous monitoring of marker release which is measured as an increase in fluorescence upon rapid dilution and dequenching of the dye in the extravesicular medium [10,11]. Under conditions resulting in less than 100% dye release, further analysis of the dye concentration remaining in liposomes after treatment with the permea-

* The opinions or assertions contained herein are the private ones of the authors and are not to be construed as official or reflecting the views of the Department of Defense or the Uniformed Services University of the Health Sciences.

** Present address: Department of Biochemistry, The George Washington University, School of Medicine and Health Sciences, 2300 Eye St., N.W., Washington, D.C. 20037, U.S.A.

Abbreviations: LUV, large unilamellar vesicle; CF, 6-carboxyfluorescein; PBS, phosphate-buffered saline; EGTA, ethylene glycol bis(β-aminoethyl ether)-*N,N,N′,N′*-tetraacetic acid; CRT, cathode ray tube; PMT, photomultiplier tube; F_0, fluorescence of CF-loaded vesicles; F_t, fluorescence after solubilization of vesicles with Triton X-100; C5, C6, C7, C8 and C9, complement proteins comprising the membrane attack complex.

Correspondence: V.W. Hu, Department of Biochemistry, The George Washington University, School of Medicine and Health Sciences, 2300 Eye Street, N.W., Washington, D.C. 20037, U.S.A.

bility-inducing agent reveals whether the dye was released in an all-or-none fashion or in a graded manner (i.e., total vs. partial release from individual liposomes) [10]. Intrinsic fluorescence of the liposomes would be expected to increase for graded release due to partial dequenching of the dye remaining within the liposome resulting from a decrease in the concentration of entrapped dye. This determination may be useful in distinguishing a stable pore from a transient one.

Although continuous monitoring of the bulk change in fluorescence of a suspension of liposomes after addition of a membrane-perturbing or pore-forming protein can provide information regarding the kinetics of the interaction, it does not permit an evaluation of possible differences in susceptibility of liposomes which may arise from vesicle size heterogeneity within a given preparation. While small unilamellar vesicles may be separated from large unilamellar vesicles (LUVs) by column methods, gel filtration cannot resolve particles greater than about 100 nm in diameter. Thus, it has not been possible to determine whether the size of an LUV affects its interaction with and subsequent lysis by a given protein.

In this report, we describe a technique capable of distinguishing carboxyfluorescein-loaded LUVs of different sizes and of determining changes in the size distribution of the residual dye-loaded vesicles which may occur in response to a membranolytic agent if vesicles are selectively lysed on the basis of size. This analysis is done without having to physically separate the dye-containing vesicles from the empty ones. In addition, we developed another method to assess the mode of dye release (all-or-none vs. graded) from vesicles. This method is complementary to fluorometric methods established for bulk vesicle solutions [10]. We applied these methods to study the interaction of terminal complement complexes, C5–8 and C5–9, with LUVs. In particular, we were interested in the effect of vesicle size on susceptibility to complement and in the mode of dye release mediated by the C5–8 and C5–9 complexes.

Materials and Methods

Preparation of vesicles. Large unilamellar vesicles (LUVs) were prepared by the reverse phase ether evaporation method [12] and were subsequently passed through 0.4 and 0.2 μm Nuclepore filters. These vesicles were composed of dimyristoylphosphatidylcholine (Calbiochem), cholesterol (Applied Science Laboratories) and dicetyl phosphate (Sigma) in a lipid molar ratio of 4 : 3 : 1 and contained entrapped chromatographically purified [10] 6-carboxyfluorescein (CF) (Molecular Probes or Eastman) at a self-quenching concentration of 100 mM in water, adjusted to pH 7.4 with NaOH. Prior to use, the vesicles were passed over a Sephadex G-25 (Pharmacia) column eluted with PBS, pH 7.4 (5 mM sodium phosphate/150 mM NaCl) to remove extravesicular dye. The ratio of the intrinsic fluorescence (F_0) of the vesicles to the total releasable fluorescence (F_t) was 0.06, a value consistent with the entrapment of CF at 100 mM [10]. These vesicles were stable and spontaneous leakage of CF did not exceed 2% over the course of the experiments.

Sonicated vesicles of the same composition as the LUVs described above were prepared by pulsed sonication at 30 °C under a stream of N_2 (30 s at 50% full power,l 30 s off for 10 or more cycles until clarity was achieved) in 100 mM CF using a Heat Systems Ultrasonics sonicator (Model W185F) equipped with a titanium microtip probe. These vesicles were eluted with PBS through a Sephadex G-25 column to remove unencapsulated CF.

Sizing of vesicles. The size distribution of vesicles was obtained either by negative-stain electron microscopy using 2% phosphotungstic acid (pH 7.4) or by light scattering measurements using a Hiac/Royco Nicomp 370 Submicron Particle Size Analyzer. In the former method, a dilute suspension of vesicles was applied to a carbon-coated formvar grid and then the excess fluid was drained off with filter paper. A drop of 2% phosphotungstic acid was then applied for 30 s and similarly removed. The grids were examined using a Zeiss 10A transmission electron microscope. The diameters of the individual vesicles were calculated from the size of the images in the electron micrographs. For measurement of vesicle sizes with the Hiac/Royco particle size analyzer, the vesicle solutions were diluted to approx. 100 μg lipid/ml (or less) and placed within the cuvette of the analyzer. The size distribution of the vesicles was

determined from fluctuations in the intensity of scattered light caused by Brownian motion of the particles. The size distribution profiles as well as the mean vesicle size are automatically determined by the instrument. The mean vesicle size for the LUV preparations as determined by both methods agreed very well with each other (265 nm by negative-stain electron microscopy and 200–250 nm by light scattering). The mean vesicle size determined by light scattering methods for the sonicated vesicle preparations was approx. 90 nm.

Fluorescence analysis of vesicles using the Meridian ACAS 470 Fluorescence Workstation. A suspension of vesicles containing entrapped CF was applied to glass slides coated with poly(L-lysine) (Sigma) and examined under a 100× oil immersion objective using the Meridian ACAS 470 Fluorescence Workstation (Meridian Instruments; Okemos, MI). The Meridian Fluorescence Workstation is a commercially available fluorescence cell analyzer equipped with a two watt argon ion laser light source, an Olympus IMT-2 inverted microscope, a Hamamatsu R1547 photomultiplier, and an IBM AT-compatible computer for data analysis. This instrument basically allows the quantitative determination of fluorescence on or within individual cells. In the work presented, we have used this instrument to quantitate fluorescence of a water-soluble dye within vesicles. Experimental details pertaining to the specific analyses are given in the respective figure legends.

Assembly of membranolytic terminal complement complexes on LUVs. Purified complement proteins, C5, C6, C7, C8, and C9 were obtained from Cytotech (California). Lysis of CF-loaded LUVs by the terminal complement complexes C5–8 and C5–9 was accomplished by acid-activated assembly [13] of these complexes on vesicles. For these experiments, 10 μg of C5 and 6 μg of C6 were mixed and the pH was reduced to 5.5 using 0.1 M HCl and immediately returned to 7 with 0.1 M NaOH to form an activated $C56^a$ complex which could initiate assembly of the terminal complexes. The activated $C56^a$ was then added to 100 μg of lipid vesicles at 37°C. After a 10 min incubation, 5.8 μg of C7 was added and the mixture was further incubated at 37°C for an additional 5 min. The vesicles were rapidly separated from unbound proteins by passage through a 6 ml Sepharose 4B column (eluted with PBS) which was spun at 400 rpm for 15–30 s at 4°C in an IEC Centra-7R benchtop centrifuge. The eluted vesicles contained bound C5–7 complexes which remained stable and active for at least 48 h as determined by the unaltered ability of C8 and C9 to induce dye release from vesicles stored over this time period. The bound C5–7 complexes do not by themselves mediate CF release. C5–8-mediated lysis was initiated by the addition of 3 μg of C8 at 37°C to 10 μg of lipid vesicles bearing C5–7. Similarly, to initiate C5–9-mediated lysis, 3 μg of C8 and 3 μg of C9 were added to 10 μg of the above lipid vesicles at 37°C. In either case, CF release was followed to endpoint in a spectrofluorometer. The amount of dye release typically reached stable values within 15 min after addition of C8 and within 1–2 min after addition of C8 + C9. C8-mediated CF release was always less at endpoint than that induced by the combination of C8 and C9.

Fluorometric analysis of all-or-none or graded release of CF from LUVs. CF release from LUVs induced by the terminal complement complexes was monitored using an SLM 8000C spectrofluorometer with the excitation wavelength at 490 nm and the emission wavelength at 520 nm. The sample chamber was maintained at 37°C with a Lauda RM6 circulating water bath. LUVs bearing C5–7 complexes were added to a cuvette containing PBS and C8 or C8 and C9 were added to initiate CF release. After the endpoints of CF release were reached, the vesicle samples were again spun through 6 ml Sepharose columns eluted with PBS to separate the released dye from the vesicles. Aliquots of the eluted vesicles were analyzed for residual fluorescence in the absence (F_o) and presence (F_t) of Triton X-100. The calculated F_o/F_t ratios were used to determine the mode of dye release according to procedures described by Weinstein et al. [10]. No further leakage of CF from the vesicles was observed after passage of the vesicles through the minicolumn, indicating that true equilibrium of CF efflux had been achieved within the timeframe of the fluorometric dye release assay. Additional aliquots of the eluted vesicles were analyzed for fluorescence distribution using the Meridian workstation as described above.

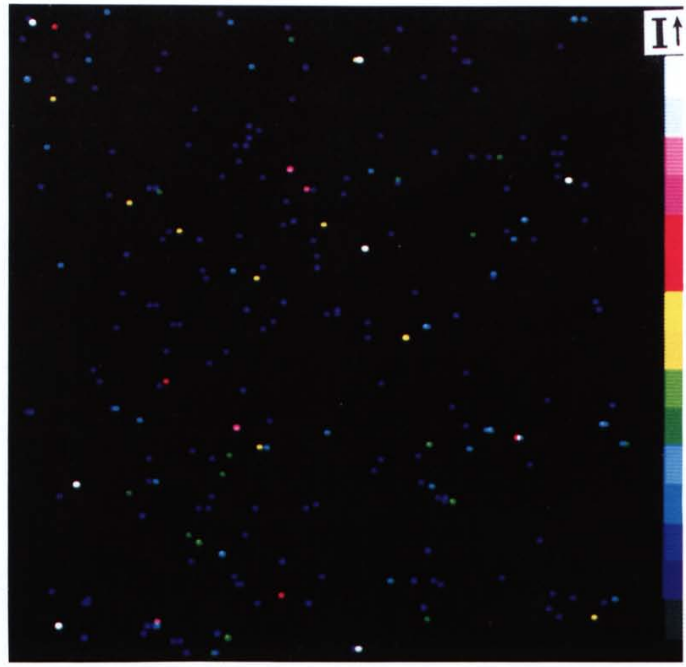

Plate I

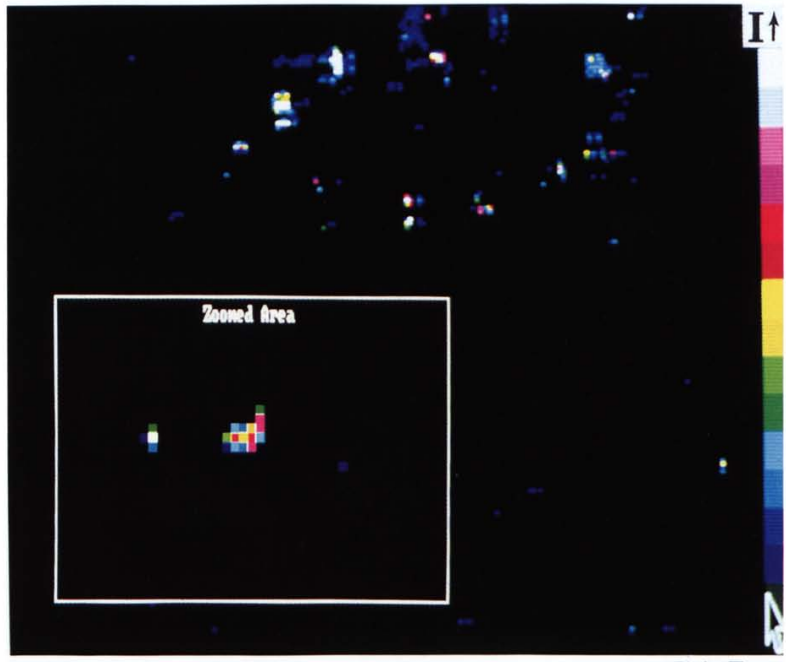

Plate II

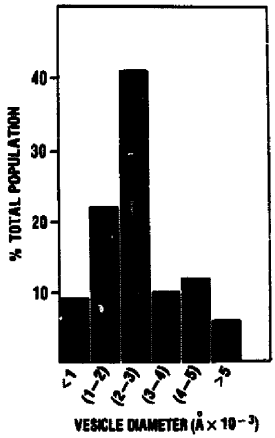

Fig. 1. Histogram showing the size distribution of CF-loaded LUVs as determined by negative-stain (phosphotungstic acid) electron microscopy. Vesicle diameters were measured on photographic plates of the images. A total of 200+ vesicles were analyzed.

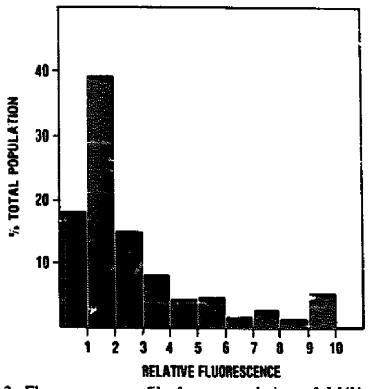

Fig. 2. Fluorescence profile for a population of LUVs. The percentage of total particles is plotted as a function of fluorescence intensity per particle (or pixel). Each division on the *x*-axis represents 15 fluorescence units. These data were obtained using the FLINT and HISTOGRAM programs of the ACAS 470 software. Instrumental parameters were as stated above. An average of 600 particles were analyzed per sample.

Results and Discussion

Relationship between vesicle size and fluorescence intensity

Negative-stain electron microscopy of CF-loaded LUV preparations shows considerable heterogeneity in vesicle size (100–1000 nm) with the mean size being ≈265 nm or 2650 Å (Fig. 1). While these dimensions are below the resolution of the light microscope, a preparation of LUVs containing 100 mM CF can be visualized on the CRT of the ACAS 470 workstation as a distribution of individual particles with fluorescence intensities which are in part dependent on the vesicle size (Plate I, p. 256). At the magnification used, each vesicle acts as a point source of light and is represented by a single fluorescent pixel, the color of which is determined by fluorescence intensity according to an arbitrary color-intensity scale. The fluorescence distribution can be more clearly demonstrated by the histogram shown in Fig. 2. By comparison with the histogram in Fig. 1 showing vesicle size distribution, it appears that particles with fluorescence intensities ranging from 16 to 30 units (39% of the population) roughly correspond to vesicles in the 200–300 nm range (41%). Furthermore, the proportion of vesicles in the 100–400 nm range (82%) is almost equivalent to the proportion of particles with fluorescence intensities ranging from 0 to 45 (80%), thus providing a semi-quantitative method of analyzing the vesicle size distribution on the basis of particle

Plate I. A population of carboxyfluorescein-loaded LUVs as seen on the CRT screen of the Meridian ACAS 470 Fluorescence Workstation. The vesicles were examined on glass slides which were coated with 0.025% poly(L-lysine) which served to anchor the vesicles as well as keep them in the same focal plane. Each vesicle is represented by a single-colored pixel. The color is a measure of fluorescence intensity. The entire field covers an area of 272160 μm^2. Each pixel corresponds to approximately 3 μm. The instrumental parameters were: PMT, 44%; X-step, 3 μm; Y-step, 3 μm; X points, 180; Y points, 168; scan strength, 6%; stage speed, 2 mm/s; laser power, 200 mW. A 90% cutoff neutral density filter was used for all experiments. Scanning the field at smaller step sizes (e.g., 0.25–1 μm) gave no evidence that any particle was greater than 1 μm in diameter.

Plate II. Ca^{2+}-induced aggregation of vesicles. Graphic representation of aggregated vesicles on the CRT screen of the ACAS 470 workstation. The inset shows a 4-fold enlargement of an aggregate using the 'zoom' feature of the ACAS 470 software. At least 50% of the particles were in clusters in the presence of 5 mM Ca^{2+}. Upon incubation with 10 mM EGTA for 1 h after Ca^{2+}-induced aggregation, only isolated pixels were observed.

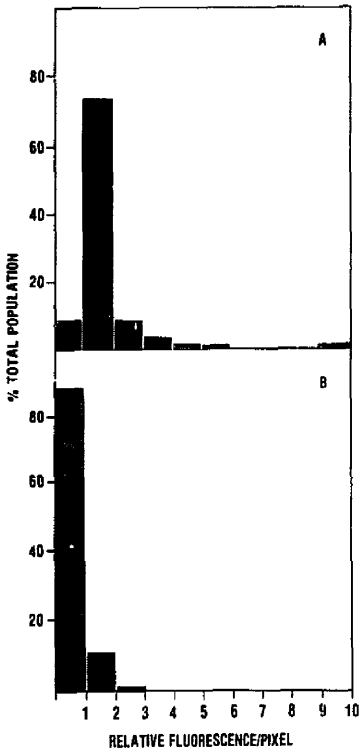

Fig. 3. Fluorescence distribution profiles of LUVs (A) and sonicated vesicles (B) obtained using the same instrumental settings. The mean fluorescence of the LUVs (mean diameter = 200 nm) was determined to be 363 and the mean fluorescence of the sonicated vesicles (mean diameter = 90 nm) was 192 in this experiment. Both sets of vesicles are loaded with 100 mM CF.

fluorescence. Additional evidence that the fluorescence of individual vesicles is dependent on vesicle size is given in Fig. 3. In comparison to LUVs (mean diameter = 200 nm) analyzed at the same instrumental settings, the fluorescence profile of smaller sonicated vesicles with a mean diameter of 90 nm is shifted towards lower intensities. As shown in Fig. 3, the major fraction of LUVs has a mean fluorescence intensity about twice as high as that of the major fraction of the sonicated vesicles. This approximately linear relationship between fluorescence intensity and vesicle diameter instead of volume probably reflects the fact that the emitted light is trivially reabsorbed at the center of the vesicle where the path length is the greatest. Alternatively, this result may also be explained by the high fluorescence intensity of dye molecules bound to the membrane as monomers. In either case, if the vesicle were large enough to be resolved, the fluorescence would appear strongest at the periphery. Thus, the overall fluorescence intensity of a single vesicle loaded with dye at a self-quenching concentration would be mostly dependent on the vesicle circumference which is a linear function of diameter. Rather than being a substitute for the more conventional methods of determining actual vesicle size (e.g., EM and light scattering), this method provides complementary information on relative vesicle size and, more importantly, allows the monitoring of changes in the size distribution of dye-loaded vesicles after reaction with a membranolytic agent (as will be shown with the C5–9 complement complex). That is, it is possible to determine whether or not there is a vesicle size preference for protein interaction within a vesicle population of predetermined size heterogeneity. This latter determination is not possible with conventional sizing methods since EM and light scattering methods cannot distinguish between dye-loaded and empty vesicles. With the method described, empty vesicles are 'invisible'.

Vesicle aggregates can be distinguished from large single vesicles

While the preceding data suggested that vesicles can be differentiated fluorometrically on the basis of size, it was important to demonstrate that particles with higher fluorescence intensities were not merely aggregates of smaller vesicles. To determine what the particles would look like under conditions favoring aggregation, Ca^{2+} was added to suspensions of negatively-charged sonicated vesicles. Plate II shows that in the presence of Ca^{2+}, clusters of colored pixels appear. Such multicolored aggregates are clearly distinct from the highly fluorescent single pixels representing individual vesicles (Plate I). Aggregation (i.e., clusters of pixels) is virtually non-existent in suspensions without Ca^{2+} and can be reversed upon addition of EGTA to Ca^{2+}-aggregated vesicles (data not shown). Thus, a population of dispersed vesicles can be readily distinguished from aggregates of vesicles. In addition, Ca^{2+}-induced aggregation of

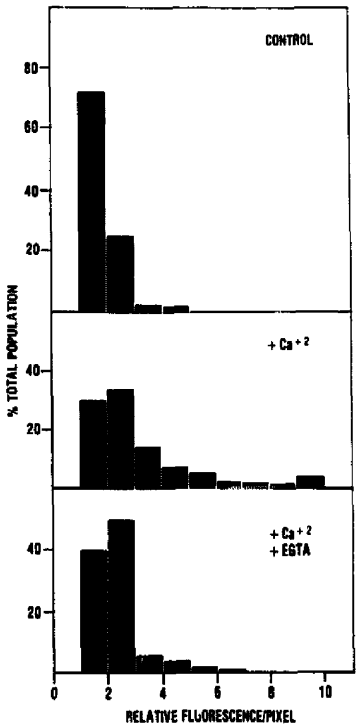

Fig. 4. Fluorescence distribution profiles for control vesicles, vesicles in the presence of 5 mM Ca^{+2}, and vesicles incubated sequentially for 1 h with 5 mM Ca^{+2} and 10 mM Mg-EGTA. As for all the previous experiments described, the fluorescence is quantitated for each pixel. Thus, the fluorescence of each pixel in an aggregate is separately determined. Fusion results in the increase of vesicle size which is consistent with the observed shift in the fluorescence distribution profile towards higher intensities/pixel relative to the control.

vesicles was accompanied by some amount of fusion. Fusion is suggested by a shift in the fluorescence distribution profile of the Ca^{2+}-treated vesicles towards higher particle (i.e., single pixel) intensities (Fig. 4). Although the addition of EGTA to Ca^{2+}-containing samples reverses aggregation such that no clusters of pixels are seen, the fluorescence distribution profile remains shifted towards higher intensities relative to the control. These observations are consistent with the net production of larger-sized particles during incubation with Ca^{2+}. Time-based fluorometric analysis of the Ca^{2+}-treated vesicles using a spectrofluorometer indicates that the fusion occurred without leakage of dye contents (data not shown).

Fluorescence distribution profile of vesicles is also dependent on entrapped dye concentration

Aside from the determination of possible changes in vesicle size distribution upon reaction with terminal complement complexes, we were interested in establishing whether the fluorescence profile of the vesicle population would change under conditions allowing the graded release of dye from vesicles. Since CF release by a graded mechanism would result in partial dequenching (and hence increased intrinsic fluorescence) of the dye remaining entrapped within vesicles after marker release had reached an endpoint, we asked whether a population of vesicles with a lower concentration of entrapped dye could be distinguished from a population of vesicles containing a higher concentration of quenched dye. For this experiment, we prepared LUVs containing 100 mM CF and 30 mM CF in which CF fluorescence is 91% and 74% quenched, respectively (Ref. 10; Solow, R., unpublished data). As shown in Fig. 5, the fluorescence of the vesicles containing 30 mM CF in notably higher than the fluorescence of the vesicles containing 100 mM CF when analyzed at the same instrument settings. This is despite the fact that the size heterogeneity of the

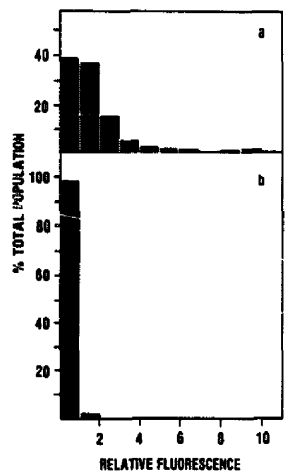

Fig. 5. Fluorescence profiles of (a) LUVs containing 30 mM CF and (b) LUVs containing 100 mM CF.

100 mM CF vesicles is nearly identical to that of the 30 mM CF vesicles. Therefore, a decrease in entrapped dye concentration caused by graded release from individual vesicles containing highly quenched dye would be expected to result in an upward shift in the overall fluorescence profile of a given vesicle population, provided that the same instrument parameters are used throughout the analysis.

Effect of membranolytic terminal complement complexes on the intrinsic fluorescence of LUVs

Lysis of CF-loaded LUVs by the terminal complement complexes C5–8 and C5–9 was accomplished by acid-activated assembly [13] of these complexes on vesicles. The progress of CF release was monitored fluorometrically as described in Methods. After marker release had reached an endpoint, the vesicles were separated from free dye by centrifugation through a Sepharose 4B minicolumn and then analyzed for residual fluorescence both in the absence (F_o) and presence (F_t) of Triton X-100 to determine the concentration of the remaining entrapped CF. An F_o/F_t ratio equivalent to that of the control preparation would indicate no change in trapped dye concentration and an 'all-or-none' process involving total dye release from affected vesicles. In contrast, a 'graded release' process is indicated by an F_o/F_t ratio higher than the control as a result of the decrease in trapped dye concentration and subsequent fluorescence dequenching of the remaining entrapped dye. As shown in Table I, C5–8-mediated lysis of LUVs was accompanied by an increase in the F_o/F_t ratio relative to the control preparation whereas the F_o/F_t ratio of

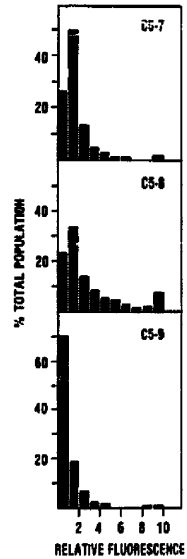

Fig. 6. Fluorescence profiles of LUVs with C5–7 complexes, C5–8 complexes, and C5–9 complexes. The PMT setting for this set of experiments was increased to 51% for greater sensitivity.

vesicles treated with C5–9 was essentially the same as the control. These results indicate that CF is released in a graded manner from C5–8-treated vesicles and in an all-or-none fashion from C5–9 vesicles. When these vesicles (after separation from released dye) were examined with the ACAS 470 fluorescence workstation, the predicted change in the fluorescence intensity profile towards a greater proportion of more fluorescent particles relative to the C5–7 control was observed for C5–8-treated vesicles (Fig. 6). This increase occurs without a

TABLE I

INTERNAL FLUORESCENCE AFTER CF RELEASE FROM LUVs INDUCED BY C5-8 AND C5-9

Sample	% CF release [a]	Predicted F_o/F_t for all-or none	Predicted F_o/F_t for graded release [b]	Measured F_o/F_t
C5–7	0 (control)	–	–	0.06±0.01
C5–8	22	0.06	0.095	0.10±0.01
C5–9	32	0.06	0.11	0.05±0.01

[a] Determined by following CF release to endpoint on a spectrofluorometer. 100% release is determined in the presence of Triton X-100.

[b] Predicted on the basis of a quenching curve determined as described in Ref. 10.

concomitant decrease in the number of particles per field, suggesting that the cause of the shift towards more highly fluorescent particles is dequenching of the dye within individual vesicles and not vesicle fusion. Data obtained with the ACAS 470 workstation thus corroborate that obtained fluorometrically and moreover show the increase in intrinsic fluorescence at the level of individual vesicles. The results of these analyses indicate that the C5–8 complex does not form a stable pore or lesion in the vesicle membrane since CF efflux ceases before equilibrium is established, resulting in sealed vesicles containing less than the original concentration of entrapped dye. These results have been confirmed using vesicles containing both CF and sucrose which achieves the same endpoint release value as CF (Solow, R., unpublished data). At present, it is difficult to explain why dye efflux from the C5–8 lesion does not achieve thermodynamic equilibrium. If the C5–8 complex forms a structural channel, the events leading to channel closing in this vesicle system are unclear. In a study using black lipid membranes, the ionic conductance induced by the C5b–8 complex was reportedly dependent on the polarity of the applied voltage while that induced by the C5b–9 complex was not [14]. In this respect, it is possible that CF efflux from a vesicle could result in a change in membrane potential which closes or alters the C5–8 channel. Alternatively, the data could be interpreted in terms of a transient destabilization of bilayer structure during insertion of C8 which results in leakage of dye. The distinction between these two possibilities requires further investigation. In contrast, the C5–9 complex forms a stable channel within the timeframe of these experiments, such that total CF release from a given vesicle can occur.

Effect of vesicle size on the susceptibility to complement attack

In contrast to data obtained with C5–8-treated vesicles, CF release from LUVs treated with C5–9 results in an overall decrease in the number of fluorescent vesicles/field examined even though the lipid concentration of the C5–9 vesicle samples examined was equivalent to that of the C5–7 and C5–8 samples. This decrease in the density of fluorescent particles was consistent with the data obtained fluorometrically on bulk vesicle solutions which indicated that vesicles with active C5–9 complexes released dye in an all-or-none manner. Thus, vesicles damaged by C5–9 were empty of dye and consequently invisible on the ACAS 470 fluorescence workstation. Interestingly, the decrease in the number of fluorescent vesicles was accompanied by a shift in the fluorescence distribution of the remaining dye-containing vesicles towards the lowest intensity or smallest particles, suggesting that the smallest vesicles within the population were preferentially spared (Fig. 6). If there were absolutely no vesicle size preference with respect to C5–9 channel formation, the fluorescence distribution profile should be the same as for the C5–7 control, even though the overall number of fluorescent particles would be smaller as a result of total dye release from affected vesicles. As expected, light scattering analysis of the C5–9 vesicle population showed no difference in size distribution from the C5–7 control since both dye-loaded and empty vesicles contributed to the size analysis (data not shown).

Conclusion

Using a digitalized fluorescence imaging method, we have shown that carboxyfluorescein-loaded vesicles can be visualized as individual colored pixels with fluorescence intensities which are dependent in part on vesicle size. In addition, we have shown that the aggregation state of these vesicles can be monitored by this method. Fusion as well as graded leakage of dye from these vesicles both lead to a shift in the fluorescence distribution profile towards particles of higher fluorescence intensities but these two phenomena may be distinguished by additional assessment of the number of fluorescent particles per field and CF leakage into the medium. Although exact vesicle size determinations cannot be made, the primary advantage of this method is the ability to determine whether dye-loaded vesicles (whose size heterogeneity has been determined by other means) are selectively damaged by membrane-perturbing or channel-forming proteins on the basis of size. Other methods for determining vesicle size distributions such as electron microscopy and light scattering methods cannot be used for this

determination since they cannot distinguish dye-loaded vesicles from empty ones. Using this method, we determined that the terminal complexes preferentially attacked medium and larger-sized vesicles (i.e., $\geqslant 200$ nm in diameter). With respect to complement-mediated membrane permeability changes, we have identified two modes of dye release. The C5–8 complex mediated a graded release of dye from vesicles whereas C5–9 releases dye in an all-or-none manner. These results suggest that, in contrast to the C5–9 complex, the C5–8 complex forms an unstable pore on lipid vesicles which closes before CF efflux reaches equilibrium values. This could also be interpreted as a transient perturbation of membrane structure by the C5–8 complex.

Acknowledgements

We thank Drs. Robert Blumenthal, Jack Holland, and Gui-sen Jiang for helpful comments and discussions. Comments by one of the reviewers were also particularly helpful. This work was in part supported by the Uniformed Services University of the Health Sciences MAALT Protocol No. GM7161 and the National Institutes of Health Grant No. R01 GM37784.

References

1 Weinstein, J.N., Yoshikami, S., Henkart, P., Blumenthal, R. and Hagins, W.A. (1977) Science 195, 489–492.
2 Blumenthal, R., Weinstein, J.N., Sharrow, S.O. and Henkart, P. (1977) Proc. Natl. Acad. Sci. USA 74, 5603–5607.
3 Weinstein, J.N., Blumenthal, R., Sharrow, S.O. and Henkart, P. (1978) Biochim. Biophys. Acta 509, 272–288.
4 Leserman, L.D., Weinstein, J.N., Blumenthal, R., Sharrow, S.O. and Terry, W.D. (1979) J. Immunol. 122, 585–591.
5 Szoka, F.C., Jacobsen, K. and Papahadjopoulos, D. (1979) Biochim. Biophys. Acta 551, 295–303.
6 Wilschut, J. and Papahadjopoulos, D. (1979) Nature 281, 690–692.
7 Hu, V.W., Esser, A.F., Podack, E.R. and Wisnieski, B.J. (1981) J. Immunol. 127, 380–386.
8 Blumenthal, R., Millard, P.J., Henkart, M.P., Reynolds, C.W. and Henkart, P.A. (1984) Proc. Natl. Acad. Sci. USA 81, 5551–5555.
9 Hu, V.W. (1986) J. Cell. Biochem., Suppl. 10B, 65.
10 Weinstein, J.N., Ralston, E., Leserman, L.D., Klausner, R.D., Dragsten, P., Henkart, P. and Blumenthal, R. (1984) in Liposome Technology (Gregoriadis, G., ed.), Vol. 3, pp. 183–204, CRC Press, Boca Raton, FL.
11 Lelkes, P.I. (1984) in Liposome Technology (Gregoriadis, G., ed.), Vol. 3, pp. 225–246, CRC Press, Boca Raton, FL.
12 Szoka, F., Olson, F., Heath, T., Vail, W., Mayhew, E. and Papahadjopoulos, D. (1980) Biochim. Biophys. Acta 601, 559–571.
13 Hansch, G.M., Hammer, C.H., Mayer, M.M. and Shin, M.L. (1981) J. Immunol. 127, 999–1002.
14 Michaels, D.W., Abramovitz, A.S., Hammer, C.H. and Mayer, M.M. (1976) Proc. Natl. Acad. Sci. USA 73, 2852–2856.